

A NEW MULTIPOINT SYMMETRIC SECANT METHOD WITH A DENSE INITIAL MATRIX

JENNIFER B. ERWAY AND MOSTAFA REZAPOUR

ABSTRACT. In large-scale optimization, when either forming or storing Hessian matrices are prohibitively expensive, quasi-Newton methods are often used in lieu of Newton’s method because they only require first-order information to approximate the true Hessian. Multipoint symmetric secant (MSS) methods can be thought of as generalizations of quasi-Newton methods in that they attempt to impose additional requirements on their approximation of the Hessian. Given an initial Hessian approximation, MSS methods generate a sequence of matrices using rank-2 updates. For practical reasons, up to now, the initialization has been a constant multiple of the identity matrix. In this paper, we propose a new limited-memory MSS method that allows for dense initializations. Numerical results on the CUTEst test problems suggest that the MSS method using a dense initialization outperforms the standard initialization. Numerical results also suggest that this approach is competitive with a basic L-SR1 trust-region method.

DEDICATION

This paper is dedicated to Oleg Burdakov who passed away June 1, 2021.

1. INTRODUCTION

We consider large-scale unconstrained optimization problems of the form

$$\min f(x), \quad (1)$$

where $f : \mathbb{R}^n \rightarrow \mathbb{R}$ is a twice-continuously differentiable function. In this setting, second-order methods are undesirable when the Hessian is too computationally expensive to compute or store. In this paper, we consider the first-order multipoint symmetric secant (MSS) method [1] and its limited-memory extension [2]. We propose a new formulation of the limited-memory MSS method that allows for a dense initialization in place of the usual scalar multiple of the identity matrix. The dense initialization does not significantly increase storage costs; in fact, the dense initialization only requires storing one extra scalar.

Multipoint symmetric secant methods can be thought of generalizations of quasi-Newton methods. Quasi-Newton methods generate a sequence of matrices $\{B_k\}$ to approximate the true Hessian of f . These methods build Hessian approximations using *quasi-Newton pairs* $\{s_k, y_k\}$ that satisfy the *secant condition* $B_{k+1}s_k = y_k$ for all k . In contrast, MSS methods seek to impose the secant condition on *all* the stored pairs: $B_k S_k = Y_k$ for all k , where

$$S_k = [s_{k-1} \ s_{k-2} \ \dots \ s_0] \quad \text{and} \quad Y_k = [y_{k-1} \ y_{k-2} \ \dots \ y_0].$$

Key words and phrases. Quasi-Newton methods; large-scale optimization; nonlinear optimization; trust-region methods .

J. B. Erway is supported in part by National Science Foundation grant IIS-1741264.

It turns out that imposing this requirement while insisting B_k is a symmetric matrix is, generally speaking, not possible. The need to relax these conditions becomes apparent when one considers that if $B_k S_k = Y_k$ then it follows that $S_k^T B_k S_k = S_k^T Y_k$, giving that $S_k^T Y_k$ must be symmetric [3]. Unfortunately, $S_k^T Y_k$ is usually not symmetric. Instead of strictly imposing both the multiple secant conditions and symmetry, some of these conditions must be relaxed.

One way to relax these conditions is to ensure the multiple secant conditions hold but not enforce symmetry. In [3], Schnabel generalizes the Powell-Symmetric-Broyden (PSB), Broyden-Fletcher-Goldfarb-Shanno (BFGS), and the Davidon-Fletcher-Powell (DFP) updates to satisfy $B_k S_k = Y_k$. However, in each case, these generalizations may not be symmetric and there are conditions that must be met for the updates to be well-defined. Alternatively, one may relax the multiple secant equations but enforce symmetry. An example of this is found in the same paper when Schnabel proposes perturbing Y_k to obtain a symmetric matrix.

Another type of relaxation takes the form of an approximation of the true $S_k^T Y_k$ using a symmetrization of this matrix. In [1], the following symmetrization is proposed:

$$\text{sym}(A) = \begin{cases} A_{i,j}, & i \geq j \\ A_{j,i}, & i < j. \end{cases}$$

With this symmetrization, a (MSS) method (and its limited-memory version described in [2]) is a symmetric method, generating a sequence of symmetric Hessian approximations. (For more details on this symmetrization, see [1, 2].) A crucial aspect of these MSS methods is that they generate a sequence of matrices that are not necessarily positive definite. It is for this reason that these methods are incorporated into trust-region methods. The update formula found in [1, 2] is a rank-2 update formula. As with traditional quasi-Newton methods, in order to maintain the low-memory advantages of limited-memory versions of the methods, a scalar multiple of the identity matrix is used to initialize the sequence of matrices. (For the duration of the paper, this initialization will be referred to as a “one-parameter initialization,” with the parameter being the chosen as a scalar.)

In this paper, we propose using a *compact formulation* for the sequence of matrices produced by the MSS method found in [1, 2] to allow the use of two parameters to define the initial approximate Hessian. This initialization exploits the form of the compact formulation to create a dense initialization when the two parameters are different. (It is worth noting that when the two parameters are chosen to be the same, the initialization simplifies to the traditional one-parameter initialization.) This work is inspired by the positive results found using a two-parameter initialization for the BFGS update [4]. We demonstrate that the eigenspace associated all the eigenvalues are unchanged using two parameters in lieu of the usual single parameter. Additionally, some motivation for good choices of initial parameters are presented.

This paper is organized in five sections. In Section 2, we review the compact formulation for the limited-memory MSS matrix. In Section 3, we derive the proposed limited-memory MSS method. This proposed method is incorporated into a traditional trust-region method in Section 4. Numerical comparisons with the MSS method using traditional initializations on large unconstrained problems from the CUTEst test collection [5] are given in Section 5. Finally, Section 6 includes some concluding remarks and observations.

1.1. Notation and Glossary. Unless explicitly indicated, $\|\cdot\|$ denotes the Euclidean two-norm or its subordinate matrix norm. The symbol e_i denotes the i^{th} canonical basis vector whose dimension depends on context.

1.2. Acknowledgment. The idea to use a dense initialization for the MSS method is due to Oleg Burdakov. An initial conversation with him about this work occurred in early 2021 and several follow-up emails were exchanged. Unfortunately, Oleg passed away before the first draft of this paper was written. We dedicate this paper to him.

2. BACKGROUND

In this section, we review how MSS matrices have been constructed, their compact formulation, and a brief overview of how they can be used in MSS methods for unconstrained optimization.

2.1. MSS matrices. Given a sequence of iterates $\{x_i\}$, we define

$$S_k = [s_{k-1} \ s_{k-2} \ \dots \ s_0] \quad \text{and} \quad Y_k = [y_{k-1} \ y_{k-2} \ \dots \ y_0], \quad (2)$$

where $s_i \triangleq x_{i+1} - x_i$ and $y_i \triangleq \nabla f(x_{i+1}) - \nabla f(x_i)$ for $i = 0, \dots, k$. For simplicity we assume S_k has full column rank. (The case when it does not have full column rank is discussed in Section 5.) The multiple secant conditions used to define a multipoint symmetric secant method are

$$B_k S_k = Y_k. \quad (3)$$

As noted in the introduction both symmetry and the multiple secant conditions cannot usually be enforced. In this work, the multiple secant conditions are relaxed by applying the symmetrization transformation [1, 2, 6]:

$$\text{sym}(A) = \begin{cases} A_{ij} & \text{if } i \geq j, \\ A_{ji} & \text{if } i < j, \end{cases} \quad (4)$$

to $S_k^T Y_k$ to guarantee symmetry. Suppose we write

$$S_k^T Y_k = L_k + E_k + T_k, \quad (5)$$

where L_k is a strictly lower triangular, E_k is the diagonal of $S_k^T Y_k$, and T_k is a strictly upper triangular matrix. With this notation, $\text{sym}(S_k^T Y_k) = L_k + E_k + L_k^T$.

With this relaxation, the recursion formula to generate MSS matrices is a rank-2 formula given by

$$B_{k+1} = B_k + \frac{(y_k - B_k s_k) c_k^T + c_k (y_k - B_k s_k)^T}{s_k^T c_k} - \frac{(y_k - B_k s_k)^T s_k c_k c_k^T}{(s_k^T c_k)^2}, \quad (6)$$

where $c_k \in \mathbb{R}^n$ is any vector such that $c_k^T s_i = 0$ for all $0 \leq i < k$ and $c_k^T s_k \neq 0$ [1]. Interestingly, if c is replaced by αc for any $\alpha \neq 0$, B_{k+1} in (6) does not change [1]. Thus, B_{k+1} is invariant with respect to the scaling of c . It can be shown that the (MSS) matrix B_k satisfies

$$S_k^T B_k S_k = \text{sym}(S_k^T Y_k), \quad (7)$$

for all $0 < k \leq n$ (see [6]). The choice of the vectors $\{c_k\}$ are not unique, and thus, the sequence $\{B_k\}$ is not unique. In [2, 6], the following choice is made for c_k so that $\{B_k\}$ satisfies a least-change problem:

$$c_k \triangleq \left[I - S_k (S_k^T S_k)^{-1} S_k^T \right] s_k.$$

For the duration of this paper, we assume this choice for $\{c_k\}$. For more details, see [1, 2]. In the following lemma, we show that despite the relaxation, the original secant condition is still satisfied.

Lemma 1. *MSS matrices satisfy the secant condition $B_{k+1}s_k = y_k$.*

Proof. Lemma 1 The proof makes use of the rank-2 formula (6):

$$\begin{aligned} B_{k+1}s_k &= \left[B_k + \frac{(y_k - B_k s_k)c_k^T + c_k(y_k - B_k s_k)^T}{s_k^T c_k} - \frac{(y_k - B_k s_k)^T s_k c_k c_k^T}{(s_k^T c_k)^2} \right] s_k \\ &\quad B_k s_k + \frac{(y_k - B_k s_k)c_k^T s_k + c_k(y_k - B_k s_k)^T s_k}{s_k^T c_k} - \frac{(y_k - B_k s_k)^T s_k c_k c_k^T s_k}{(s_k^T c_k)^2} \\ &= B_k s_k + (y_k - B_k s_k) + \frac{c_k(y_k - B_k s_k)^T s_k}{s_k^T c_k} - \frac{(y_k - B_k s_k)^T s_k c_k}{(s_k^T c_k)} \\ &= y_k. \end{aligned}$$

□

2.2. Compact formulation and the limited-memory case. Given an initial B_0 , Brust [6] derives the compact formulation $B_k = B_0 + \Psi_k M_k \Psi_k^T$, where

$$\Psi_k \triangleq \begin{bmatrix} S_k & (Y_k - B_0 S_k) \end{bmatrix} \quad \text{and} \quad M_k \triangleq \begin{bmatrix} W(S_k^T B_0 S_k - (T_k + E_k + T_k^T))W & W \\ W & 0 \end{bmatrix}, \quad (8)$$

$W \triangleq (S_k^T S_k)^{-1}$, and L_k , E_k , and T_k are defined as in (5). It is worth noting that $B_0 S$ in (8) is not difficult to compute when B_0 is the dense matrix proposed in this paper (see Section 5 for details).

Limited-memory MSS matrices are obtained by storing no more than m of the most recently-computed quasi-Newton pairs. As in all limited-memory quasi-Newton methods, m is typically less than 10 (e.g., Byrd et al. [7] suggest $m \in [3, 7]$). In this case, the compact formulation given in (8) holds but with S_k and Y_k defined to contain at most m vectors where $m \ll n$, i.e.,

$$S_k = [s_{k-1} \ s_{k-2} \ \dots \ s_{k-l}] \in \Re^{n \times l} \quad \text{and} \quad Y_k = [y_{k-1} \ y_{k-2} \ \dots \ y_{k-l}] \in \Re^{n \times l}, \quad (9)$$

where $l \leq m$. In the compact representation (8), M_k is at most size $2m \times 2m$, making it a small enough matrix to perform linear algebra operations that are ill-suited for larger (e.g., $n \times n$) matrices. For the duration of the paper, we assume the MSS method is the limited-memory version where S_k and Y_k are defined by (9).

2.3. MSS methods. The MSS matrices used in this work have been proposed to solve systems of equations [1], bound constrained optimization problems [2], and unconstrained optimization [6] problems. In this section, we review how they can be used to solve (1).

Because MSS matrices can be indefinite, it is natural to use this sequence of matrices as approximations to the true Hessian in a trust-region method. We briefly review trust-region methods here, but further details can be found in standard optimization textbooks (see, e.g., [8]).

At each iterate, trust-region methods use a quadratic approximation m_k to model f at the current iterate in a small region neighborhood about the current iterate x_k :

$$m_k(x_k + s) = f(x_k) + g_k^T s + \frac{1}{2} s^T B_k s, \quad (10)$$

where $g_k = \nabla f(x_k)$ and $B_k \approx \nabla^2 f(x_k)$. At each iteration, trust-region methods solve the so-called *trust-region subproblem* to obtain a new search direction s_k :

$$s_k = \arg \min_{\substack{s \in \mathbb{R}^n \\ \|s\| \leq \Delta_k}} Q(s) = g_k^T s + \frac{1}{2} s^T B_k s, \quad (11)$$

where Δ_k is the trust-region radius and $\|\cdot\|$ is any vector norm. Having obtained a search direction s_k , a basic trust-region algorithm computes a new iterate $x_{k+1} = x_k + s_k$, provided s_k satisfies a sufficient decrease criteria. (For more details, see, e.g., [8, 9].)

One of the advantages of using the Euclidean norm to define the trust region is that the subproblem is guaranteed to have an optimal solution. The following theorem [10, 11] classifies a global solution to the trust-region subproblem defined using the Euclidean norm:

Theorem 1. *Let Δ be a positive constant. A vector p^* is a global solution of the trust-region subproblem (11) where $\|\cdot\|$ is the Euclidean norm if and only if $\|p^*\| \leq \Delta$ and there exists a unique $\sigma^* \geq 0$ such that $B + \sigma^* I$ is positive semidefinite and*

$$(B + \sigma^* I)p^* = -g \quad \text{and} \quad \sigma^*(\Delta - \|p^*\|_2) = 0. \quad (12)$$

Moreover, if $B + \sigma^* I$ is positive definite, then the global minimizer is unique.

It should be noted that these optimality conditions also serve as the basis for some algorithms to find the solution to subproblems defined by the Euclidean. Specifically, these algorithms find an optimal solution by searching for a point that satisfies the conditions given in (12) (see, e.g., [11, 12, 13, 14].)

The MSS method proposed in this paper uses a trust-region method defined by the Euclidean norm. The method solves each trust-region subproblem using the ideas in [14] for solving indefinite subproblems. The following section overviews these ideas.

2.4. The Orthonormal basis L-SR1 (OBS) method. The OBS method [14] is a trust-region method for solving limited-memory symmetric rank-one (L-SR1) trust-region subproblems. The method is able to solve subproblems to high accuracy by exploiting the optimality conditions given in Theorem 1. L-SR1 matrices are generated by a recursion relation using rank-1 updates that satisfy the secant condition $B_{k+1}s_k = y_k$ for all k . Importantly, as with MSS matrices, L-SR1 matrices can be indefinite. (For details on L-SR1 matrices and methods see, e.g., [8].)

The OBS method makes use of the partial spectral decomposition that can be computed efficiently from the compact formulation [13, 14, 15]. In particular, suppose the compact formulation of an L-SR1 matrix B_{k+1} is given by $B_{k+1} = B_0 + \Psi M \Psi^T$, with $B_0 = \gamma I$. Further, suppose $\Psi = QR$ is the “thin” QR factorization of Ψ where $Q \in \mathbb{R}^{n \times (k+1)}$ and $R \in \mathbb{R}^{(k+1) \times (k+1)}$ is invertible. Then,

$$B_{k+1} = \gamma I + QRM R^T Q^T,$$

where RMR^T is a small $(k+1) \times (k+1)$ matrix (i.e., the number of stored quasi-Newton pairs is $k+1$.) Given the spectral decomposition $U\hat{\Lambda}U^T$ of RMR^T , the spectral decomposition of B_{k+1} can be written as $B_{k+1} = P\Lambda P^T$, where

$$\Lambda \triangleq \begin{bmatrix} \hat{\Lambda} + \gamma I & 0 \\ 0 & \gamma I \end{bmatrix} \quad \text{and} \quad P \triangleq [QU \quad (QU)^\perp].$$

For more details on this derivation for the L-SR1 case, see [14].

The OBS method uses the above derivation to determine the eigenvalues of B_k at each iteration. Then, depending on the definiteness of B_k , the method computes a high-accuracy solution using the optimality conditions. In some cases, a global solution can be computed directly by formula; in other cases, Newton's method must be used to compute σ^* and then p^* is computed directly by solving $(B + \sigma I)p^* = -g$. It is worth noting that in the latter case, Newton's method can be initialized to guarantee that Newton converges monotonically without needing any safeguarding. Moreover, a high-accuracy solution can also be computed in the so-called *hard case* [14].

The OBS method can be generalized to solve trust-region subproblems where the approximation to the Hessian admits any compact representation. The addition of a second parameter to the compact formulation (e.g., the proposed dense initialization) requires significant modifications to the code. However, the resulting code makes use of the same strategy as the OBS method. The partial spectral decomposition of a MSS matrix is carefully presented in the following section.

3. THE DENSE INITIALIZATION

In this section, we propose a MSS method with a dense initialization. In order to introduce the dense initialization, we begin by demonstrating how to compute a partial spectral decomposition of an MSS matrix in order to lay the groundwork for the dense initialization.

3.1. The spectral decomposition. Recall the compact formulation of a MSS matrix:

$$B_k = B_0 + \Psi_k M_k \Psi_k^T, \quad (13)$$

where

$$\Psi_k \triangleq [S_k \quad (Y_k - B_0 S_k)] \quad \text{and} \quad M_k \triangleq \begin{bmatrix} W(S_k^T B_0 S_k - (T_k + E_k + T_k^T))W & W \\ W & 0 \end{bmatrix}, \quad (14)$$

$W \triangleq (S_k^T S_k)^{-1}$, and L_k , E_k , and T_k are defined as in (5). Note that this factorization does not require B_0 is a scalar multiple of the identity matrix. We assume that $\Psi_k \in \mathbb{R}^{n \times 2l}$ and $M_k \in \mathbb{R}^{2l \times 2l}$ where $l \leq m$, and m is the maximum number of stored quasi-Newton pairs.

For this derivation of the partial spectral decomposition of B_k , we assume $B_0 = \gamma I$ for simplicity. If the “thin” QR factorization of Ψ_k is $\Psi_k = QR$, where $Q \in \mathbb{R}^{n \times 2l}$ and $R \in \mathbb{R}^{2l \times 2l}$ then

$$B_k = B_0 + QRM_k R^T Q^T.$$

The matrix $RM_k R^T \in \mathbb{R}^{2l \times 2l}$ is small, and thus, its spectral decomposition can be computed in practice. Let $U\hat{\Lambda}U^T$ be the spectral decomposition of $RM_k R^T \in \mathbb{R}^{2l \times 2l}$. This gives us

$$B_k = B_0 + QU\hat{\Lambda}U^T Q^T, \quad (15)$$

and so, $B_k = P\Lambda P^T$ where

$$\Lambda \triangleq \begin{bmatrix} \hat{\Lambda} + \gamma I & 0 \\ 0 & \gamma I \end{bmatrix} \quad \text{and} \quad P \triangleq [QU \quad (QU)^\perp]. \quad (16)$$

Here, Λ is a diagonal matrix whose first $2l$ entries are $\hat{\lambda}_i + \gamma$, where $\hat{\Lambda} = \text{diag}(\hat{\lambda}_1, \dots, \hat{\lambda}_{2l})$, and the (2,2) block of Λ contains the eigenvalue γ with multiplicity $n - 2l$. The first $2l$ columns of P are made up of QU , which is orthogonal since it is the product of

two orthogonal matrices. In contrast, $(QU)^\perp \in \Re^{n \times (n-2l)}$ is very computationally expensive to compute and will never be explicitly used. Finally, provided Ψ_k has full column rank, it is worth noting that it is possible to form QU without storing Q ; namely, QU can be computed using the formula $QU = \Psi_k R^{-1} U$. For simplicity, we define $P_{\parallel} = QU$ so that $P = [P_{\parallel} \ P_{\perp}]$, where $P_{\perp} = P_{\parallel}^{\perp}$. Notice that this is the same form as the spectral decomposition in (16) but with different-sized matrices.

3.2. The dense initial matrix. In the previous subsection, we assumed that $B_0 = \gamma I$, i.e., a scalar multiple of the identity matrix. In this subsection, we show how the spectral decomposition of B_k can be used to design a two-parameter dense initialization.

Consider the spectral decomposition $B_k = P \Lambda P^T$ where Λ and P are defined in (16). In the case that $B_0 = \gamma I$, then $B_0 = \gamma P P^T$ since P is orthogonal. Moreover, B_0 can be written as

$$B_0 = \gamma_k P_{\parallel} P_{\parallel}^T + \gamma_k P_{\perp} P_{\perp}^T.$$

The dense initialization is formed by assigning a different parameter to each subspace, i.e.,

$$\tilde{B}_0 = \zeta_k P_{\parallel} P_{\parallel}^T + \zeta_k^C P_{\perp} P_{\perp}^T, \quad (17)$$

where ζ_k and ζ_k^C can be updated each iteration.

Theorem 2. *Given \tilde{B}_0 as in (17), then B_k in (13) has the following spectral decomposition:*

$$B_k = [P_{\parallel} \ P_{\perp}] \begin{bmatrix} \hat{\Lambda} + \zeta_k I & 0 \\ 0 & \zeta_k^C I \end{bmatrix} \begin{bmatrix} P_{\parallel}^T \\ P_{\perp}^T \end{bmatrix}. \quad (18)$$

Proof. Theorem 2 By (15) and (17), we have

$$\begin{aligned} B_k &= \tilde{B}_0 + \Psi_k M_k \Psi_k^T \\ &= \tilde{B}_0 + P_{\parallel} \hat{\Lambda} P_{\parallel}^T \\ &= \zeta_k P_{\parallel} P_{\parallel}^T + \zeta_k^C P_{\perp} P_{\perp}^T + P_{\parallel} \hat{\Lambda} P_{\parallel}^T \\ &= [P_{\parallel} \ P_{\perp}] \begin{bmatrix} \hat{\Lambda} + \zeta_k I & 0 \\ 0 & \zeta_k^C I \end{bmatrix} \begin{bmatrix} P_{\parallel}^T \\ P_{\perp}^T \end{bmatrix}. \end{aligned}$$

□

Corollary 1. *The eigenspace associated with the eigenvalues of B_k is not changed using the dense initialization (17) in lieu of the one-parameter initialization.*

3.3. Parameter choices. If $\zeta_k = \zeta_k^C$ then the two-parameter initialization reduces to the one-parameter initialization. In this case, one possible motivation to pick ζ_k is to better ensure that the multiple secant conditions hold, i.e., $B_k S_k = Y_k$ for all k . Thus, ζ_k can be selected to be the a solution of the following minimization problem:

$$\tilde{B}_0 = \arg \min_{B_0} \left\| B_0^{-1} Y_k - S_k \right\|_F^2, \quad (19)$$

where $\|\cdot\|_F$ denotes the Frobenius norm.

Theorem 3. *If \tilde{B}_0 is chosen to be in the form of (17) with $\zeta_k = \zeta_k^C$, then the solution to (19) is*

$$\zeta_k = \zeta_k^C = \begin{cases} \sum_{i=k-l}^{k-1} \frac{y_i^T y_i}{y_i^T s_i} & \text{if } k > 1, \\ \frac{\|y_0^T\|^2}{y_0^T s_0} & \text{if } k = 1, \end{cases} \quad (20)$$

where l is the number of stored quasi-Newton pairs.

Proof. Theorem 3 Since $\zeta_k = \zeta_k^C$, the initialization is a one-parameter initialization, and thus, the solution to (19) is of the form $\tilde{B}_0 = \zeta_k I$. Substituting this into (19) gives that

$$\zeta_k = \arg \min_{\zeta_k} \left\| \zeta_k^{-1} Y_k - S_k \right\|_F^2. \quad (21)$$

Using properties of the trace we have the following:

$$\begin{aligned} \zeta_k &= \arg \min_{\zeta} \left\| \zeta^{-1} Y_k - S_k \right\|_F^2 \\ &= \arg \min_{\zeta} \text{trace} \left((\zeta^{-1} Y_k - S_k)^T (\zeta^{-1} Y_k - S_k) \right) \\ &= \arg \min_{\zeta} \sum_{i=k-l}^{k-1} \left((\zeta^{-1} y_i - s_i)^T (\zeta^{-1} y_i - s_i) \right) \\ &= \sum_{i=k-l}^{k-1} \frac{2y_i^T y_i}{y_i^T s_i + s_i^T y_i} \\ &= \sum_{i=k-l}^{k-1} \frac{y_i^T y_i}{y_i^T s_i}. \end{aligned} \quad (22)$$

Note that if $l = 1$, then

$$\zeta_k = \zeta_k^C = \frac{\|y_{k-1}^T\|^2}{y_{k-1}^T s_{k-1}} = \gamma_{k-1}, \quad (23)$$

which is the conventional initialization for the BFGS method and sometimes referred to as the Barzilai and Borwein (BB) initialization [16]. \square

We now consider choices for the two-parameter dense initialization. The following theorem shows that once ζ_k is fixed then there is an analytical solution to (19). However, before stating the theorem, we prove the following lemma.

Lemma 2. *The following relationships hold between S_k , Ψ_k and P_{\parallel} : (i) $\text{Range}(S_k) \subseteq \text{Range}(\Psi_k)$, (ii) $\text{Range}(S_k) \subseteq \text{Range}(P_{\parallel})$, and (iii) $P_{\parallel} P_{\parallel}^T S_k = S_k$.*

Proof. Lemma 2 Since $\Psi_k = [S_k \ Y_k - B_0 S_k]$ it follows immediately that $\text{Range}(S_k) \subseteq \text{Range}(\Psi_k)$. Note that $P_{\parallel} = \Psi_k R^{-1} U$, it follows that $\text{Range}(\Psi_k) = \text{Range}(P_{\parallel})$. Finally, $P_{\parallel} P_{\parallel}^T S_k = S_k$ since $\text{Range}(S_k) \subseteq \text{Range}(P_{\parallel})$. \square

Theorem 4. *Suppose \tilde{B}_0 as in (17). Then, for a fixed ζ_k^C , the optimal solution to*

$$\zeta_k = \arg \min_{\zeta} \left\| \tilde{B}_0^{-1} Y_k - S_k \right\|_F^2, \quad (24)$$

where $\|\cdot\|_F$ denotes the Frobenius norm, is given by

$$\zeta_k = \frac{\text{tr}(Y_k^T Y_k)}{2\text{tr}(Y_k^T S_k)}.$$

Proof. Theorem 4 Let

$$\zeta_k = \arg \min_{\zeta} \left\| \left(\zeta^{-1} P_{\parallel} P_{\parallel}^T + (\zeta_k^C)^{-1} P_{\perp} P_{\perp}^T \right) Y_k - S_k \right\|_F^2. \quad (25)$$

Notice that the right-hand side of (25) is equivalent to

$$\text{tr} \left(\left(\zeta^{-1} P_{\parallel} P_{\parallel}^T Y_k + (\zeta_k^C)^{-1} P_{\perp} P_{\perp}^T Y_k - S_k \right)^T \left(\zeta^{-1} P_{\parallel} P_{\parallel}^T Y_k + (\zeta_k^C)^{-1} P_{\perp} P_{\perp}^T Y_k - S_k \right) \right), \quad (26)$$

where “tr” denotes the trace operator. Using properties of the trace and orthogonal projectors, together with Lemma 2, (26) is equivalent to

$$\frac{1}{\zeta^2} \text{tr}(Y_k^T P_{\parallel} P_{\parallel}^T Y_k) - \frac{2}{\zeta} \text{tr}(Y_k^T S_k) + \frac{1}{(\zeta_k^C)^2} \text{tr}(Y_k^T P_{\perp} P_{\perp}^T Y_k) + \text{tr}(S_k^T S_k). \quad (27)$$

To compute the minimizer of (25), we differentiate (26) with respect to ζ to obtain:

$$-\frac{1}{\zeta^3} \text{tr}(Y_k^T P_{\parallel} P_{\parallel}^T Y_k) + \frac{2}{\zeta^2} \text{tr}(Y_k^T S_k). \quad (28)$$

Since $P_{\parallel} P_{\parallel}^T$ is an orthogonal projector, we have by properties of the trace and Frobenius norm that

$$\text{tr}(Y_k^T P_{\parallel} P_{\parallel}^T Y_k) = \text{tr}(P_{\parallel} P_{\parallel}^T Y_k Y_k^T) = \|P_{\parallel} P_{\parallel}^T Y_k Y_k^T\|_F^2 = \|Y_k Y_k^T\|_F^2 = \text{tr}(Y_k Y_k^T) = \text{tr}(Y_k^T Y_k).$$

Substituting into (28), setting the result equal to zero, and solving for ζ yields:

$$\zeta_k = \frac{\text{tr}(Y_k^T Y_k)}{2\text{tr}(Y_k^T S_k)}. \quad (29)$$

This is a minimizer since the equation to be minimized is convex in ζ . \square

Corollary 2. Suppose \tilde{B}_0 as in (17) and ζ_k is fixed. Then, increasing ζ_k^C will reduce $\|B_k S_k - Y_k\|_F$.

Proof. Corollary 2 This corollary is a direct result of (27). \square

Theorem 4 states that given any fixed ζ_k^C , the choice of ζ_k that minimizes the error in Frobenius norm of $B_k S_k = Y_k$ is given by (29). It is remarkable how similar this result is to the result of Theorem 3. Moreover, Corollary 2 implies that small ζ_k^C corresponds to more relaxing of the multiple secant conditions. At first glance, the first and third term in (27) suggest that both ζ_k and ζ_k^C play equal roles in the distance of $B_k S_k$ to Y_k since $\text{tr}(Y_k^T P_{\perp} P_{\perp}^T Y_k) = \text{tr}(Y_k^T P_{\parallel} P_{\parallel}^T Y_k) = \text{tr}(Y_k^T Y_k)$; however, there is an extra term in (27) that could reduce the distance from $B_k S_k$ to Y_k that only depends on ζ_k . (The corresponding term that involved ζ_k^C canceled out since $P_{\perp} P_{\perp}^T S_k = 0$.) Thus, provided $\text{tr}(Y_k^T S_k) > 0$, ζ_k reduces the contribution of first term in (27) to the distance between $B_k S_k$ and Y_k . In other words, there ζ_k is afforded a counter balance that ζ_k^C is not. This is significant because it identifies that ζ_k has more influence on the relaxation of the multiple secant equations than ζ_k^C . In other words, the eigenvalues associated with the low-dimensional eigenspace have more influence over the satisfaction of the multiple secant conditions than the eigenvalues of the large eigenspace.

It is worth noting that applying either theorem in this section could result in a choice of ζ_k that is negative. The disadvantage of negative ζ_k is that the initial B_0 will have $2l$ negative eigenvalues. While rank-2 updates could shift these eigenvalues into positive territory, the subproblem solver will need to be computing solutions on the boundary of the trust region as long as any eigenvalue of B_k is negative. This is undesirable for two reasons (i) at a local solution of (1) it is desirable that B_k is positive definite and (ii) it is more computationally expensive for the subproblem solver to compute solutions on the boundary than in the interior of the trust region.

4. THE PROPOSED MSS METHOD

In this section, we present the proposed MSS method. This method uses a trust-region method whose subproblems are defined using a MSS matrix. The result is a type of quasi-Newton trust-region method whose approximate Hessian can be indefinite at any given iteration. Finally, this section concludes with a discussion of the computational cost of the proposed method.

4.1. Ensuring S_k has full rank. In order for the compact formulation to exist, it must be the case that S_k has full rank so that $W = (S_k^T S_k)^{-1}$ in (8) is well-defined. To ensure this, the LDL^T factorization of $S_k^T S_k$ is computed to find linearly dependent columns in S_k . Specifically, small diagonal elements in D correspond to columns of S_k that are linearly dependent. Let \hat{S}_k denote the matrix S_k after removing the linearly dependent columns. The resulting matrix $\hat{W} \triangleq (\hat{S}_k^T \hat{S}_k)^{-1}$ is positive definite, and thus, invertible. This strategy is not new and was first proposed in this context in [13]. For notational simplicity, we assume that S_k has linearly independent columns for the remainder of this section because if it is not full rank, linear dependence will be removed by this procedure. For the proposed MSS method, a full rank S_k is used to define Ψ .

4.2. Ensuring Ψ has full rank. It is also desirable that Ψ is full rank to avoid any adverse affects on the condition number of B_k . If Ψ is not full rank, then $\hat{\Lambda}$ will have at least one diagonal entry that is close to zero (the number of small diagonal elements of R will correspond to the number of small eigenvalues of RMR^T). Without loss of generality, assume that i is such that $\hat{\lambda}_i + \zeta_k \approx \zeta_k$, i.e., $\hat{\lambda}_i \approx 0$. In the cases when $|\hat{\lambda}_i + \zeta_k| \approx |\zeta_k|$ is the largest or smallest approximate eigenvalue of B_k in absolute value, the condition number of B_k will be negatively affected, possibly detrimentally. In contrast, if $|\hat{\lambda}_j + \zeta_k| \leq |\zeta_k| \leq |\hat{\lambda}_{\hat{k}} + \zeta_k|$ for some $j, \hat{k} \in \{0, 1, \dots, \text{rank}(S)\}$ then the condition number of B_k will not be impacted. For this reason, ensuring that Ψ has full rank will help prevent unnecessary ill-conditioning.

In order to enforce that Ψ has full rank, we also perform the LDL^T factorization of $\Psi^T \Psi$ to find linearly dependent columns of Ψ , similar to the procedure to ensure that S_k is full rank.

4.3. LDL^T and its effect on the eigendecomposition. Using the LDL^T factorization of $\Psi^T \Psi$ in lieu of the QR factorization of Ψ in Section 3.1 requires redefining the eigendecomposition of B_k . The following presentation is based on [17].

Suppose $\Pi^T \Psi^T \Psi \Pi = LDL^T$ is the LDL^T factorization of $\Psi^T \Psi$ and Π is a permutation matrix. Let J be the set of indices such that the corresponding diagonal entry in D is sufficiently large (see Section 4.5 for the criteria). Then,

$$\Psi^T \Psi \approx \Pi L_{\dagger} D_{\dagger} L_{\dagger}^T \Pi^T = \Pi R_{\dagger}^T R_{\dagger} \Pi^T,$$

where L_{\dagger} is the matrix L having removed columns indexed by an element not in J , D_{\dagger} is the matrix D having removed any rows and columns indexed by an element not in J , $R_{\dagger} \triangleq \sqrt{D_{\dagger}}L_{\dagger}^T \in \mathbb{R}^{r \times 2(l+1)}$, and $r = |J|$. This gives the approximate decomposition of B_k :

$$B_k = B_0 + Q_{\dagger}R_{\dagger}\Pi^T M\Pi R_{\dagger}^T Q_{\dagger}^T,$$

where $Q_{\dagger} \triangleq (\Psi\Pi)_{\dagger}R_{\dagger}^{-1}$, $(\Psi\Pi)_{\dagger}$ is the matrix $\Psi\Pi$ having deleted columns not indexed in J , and R_{\dagger} is R_{\dagger} having removed columns not indexed in J . (For more details on this derivation, see [17].)

The partial eigendecomposition proceeds as in Section 3.1 but with $R_{\dagger}\Pi^T M\Pi R_{\dagger}^T$ in lieu of RMR^T . Finally, as in [17], P_{\parallel} can be computed as

$$P_{\parallel} = (\Psi\Pi)_{\dagger}R_{\dagger}^{-1}U. \quad (30)$$

4.4. MSS algorithm with a dense initial matrix. The following algorithm is the proposed MSS algorithm. Details follow the algorithm. Brackets used to denote quantities that are stored using more than one variable. (For example, $[Bp] = -g$ means to store $-g$ in the variable name Bp .) In the below algorithm, m denotes the maximum number of stored quasi-Newton pairs and l denotes the current number of stored pairs. The MSS algorithm requires an initial x as well as a way to compute the function f and its gradient g at any point.

PROCEDURE 1: MSS Method with dense initialization

```

1: Input:  $x$ 
2: Pick  $0 \ll \tau < \hat{\tau}$ ;
3: Set  $m \in [3, 7]$  with  $m \in \mathbb{Z}^+$ ,  $\Delta = 1$ ;
4: Set  $f \leftarrow f(x)$  and  $g \leftarrow g(x)$ ;  $l \leftarrow 0$ ;
5:  $p \leftarrow -g$ ; store  $[Bp] = -g$ ;
6: Update  $f$ ,  $g$ , and  $x$ ;
7: Update  $s$  and  $y$ ;  $l \leftarrow 1$ ;
8: Update  $\Delta$  using Algorithm (2);
9: while not converged do
10:   if  $l \leq m$ , then
11:     Add  $s$  to  $S$  and add  $y$  to  $Y$ ;  $l \leftarrow l + 1$ ;
12:   else
13:     Remove oldest pair in  $S$ ,  $Y$ , and corresponding column in  $\Psi$ ;
14:     Add  $s$  to  $S$  and add  $y$  to  $Y$ ;
15:   end if
16:   Compute  $\zeta$  and  $\zeta^C$  (e.g., Section 3.3); Update  $\Psi$ ;
17:   Ensure  $S$  and  $\Psi$  are full rank using Sections 4.1-4.2; Store  $R_{\dagger}$ ,  $R_{\dagger}^{-1}$ ;
18:   Update  $M$ ;
19:   Compute the spectral decomposition  $U\hat{\Lambda}U^T$  of  $R_{\dagger}\Pi^T M\Pi R_{\dagger}^T$ ;
20:    $\Lambda \leftarrow \hat{\Lambda} + \zeta I$ ;
21:   if  $\text{cond}(B) \leq \tau$  and  $\|B\| \leq \hat{\tau}$ , then
22:      $[p, Bp] = \text{obs}^*(g, \Psi, R_{\dagger}^{-1}, U, \Lambda, \zeta, \zeta^C, \Delta)$ ;
23:   else
24:      $\beta \leftarrow \min(\|g\|/\Delta, 1)$ ;  $p \leftarrow -(\beta\Delta/\|g\|)g$ ; Compute  $[Bp]$ ;
25:   end if
26:   Update  $f$ ,  $g$ , and  $x$ ;
27:   Update  $s$  and  $y$ ;
28:   Update  $\Delta$  using Algorithm (2);
29: end while
30: Output:  $x$ 

```

Algorithm 1 begins by letting $B_0 = I$, and thus, the search direction is the steepest descent direction. (Future iterations use the dense initialization.) The update to Δ at each iteration makes use of Algorithm 2, which is a standard way to update the trust-region radius (see, for example, [8]). In Algorithm 2, the variable ρ stores the ratio between the actual change and the predicted change. If this ratio is sufficiently large, then the step is accepted and the trust-region radius is possibly updated. If the ratio is too small, the step is rejected and Δ is decreased. Note that the implicit update to B_k , i.e., the acceptance of a new quasi-Newton pair (lines 7 and 25 in Algorithm 1), is independent of whether the step is accepted in Algorithm 2.

The LDL^T decomposition is used twice in line 16 in Algorithm 1. Each time, the i th diagonal entry of D is considered to be sufficiently large provided

$$D_{ii} > \text{tol} * \max_j |D_{jj}|,$$

where D_{jj} denotes the j th diagonal entry in D and tol is small positive number (see Sections 4.1-4.2 for more details).

Finally, in line (21), a modified `obs` method (denoted by the asterisk) is used to solve the trust-region subproblem provided the condition number and norm of B are reasonable. Note that since we have the eigenvalues of B , it is quick to compute the condition number. The test in line (21) prevents the algorithm from solving the subproblem when B is very ill-conditioned or $\|B\|$ is too large. In the event B is too ill-conditioned or large, p is set to be the Cauchy point computed with $B = I$. The reason for this is that in numerical experiments, attempting to compute a solution to the trust-region subproblem with very ill-conditioned matrices B led to inferior results.

PROCEDURE 2: Update the trust-region radius

```

1: Fix:  $0 < \eta_1 < \eta_2 < 1$ ,  $0 < \gamma_1, \gamma_p < 1 < \gamma_2$ ;
2:  $\rho \leftarrow (f_{\text{new}} - f) / (-g^T p - 0.5p^T[Bp], 0)$ ;
3: if  $\rho \geq \eta_1$ , then
4:    $f \leftarrow f_{\text{new}}$ ;  $x \leftarrow x + p$  and  $g \leftarrow \nabla f(x)$ ;
5:   if  $\rho \geq \eta_2$ , then
6:     if  $\|p\| > \gamma_p \Delta$ , then
7:        $\Delta \leftarrow \gamma_2 \Delta$ ;
8:     end if
9:   end if
10: else
11:    $\Delta \leftarrow \gamma_1 \Delta$ ;
12: end if

```

Theorem 5. Let $f : \mathbb{R}^n \rightarrow \mathbb{R}$ be a twice-continuously differentiable and bounded below. Suppose there exists scalars $c_1, c_2 > 0$ such that

$$\|\nabla^2 f(x)\| \leq c_1 \quad \text{and} \quad \|B_k\| \leq c_2, \quad (31)$$

for all $x \in \mathbb{R}^n$ and for all k . Consider the sequence $\{x_k\}$ generated by Algorithm 1 with $\zeta, \zeta^C \in \mathbb{R}$. Then,

$$\lim_{k \rightarrow \infty} \|\nabla f(x_k)\| = 0.$$

Proof. Theorem 5 Since the OBS method generates high-accuracy solutions to the trust-region subproblem and in the case that $\|B_k\|$ is too large the Cauchy point is used as the approximate solution, all the assumptions of Theorem 6.4.6 in [9] are met, proving convergence. \square

| | ζ_k | ζ_k^C |
|----------|--|--|
| Option 1 | $\frac{y_k^T y_k}{y_k^T s_k}$ | $\frac{y_k^T y_k}{y_k^T s_k}$ |
| Option 2 | $\sum_{k-1}^{k-l} \frac{y_i^T y_i}{y_i^T s_i}$ | $\sum_{k-1}^{k-l} \frac{y_i^T y_i}{y_i^T s_i}$ |
| Option 3 | $\frac{1}{2} \sum_{k-1}^{k-l} \frac{y_i^T y_i}{y_i^T s_i}$ | $\frac{y_k^T y_k}{y_k^T s_k}$ |
| Option 4 | $\max_{k-1 \leq i \leq k-l} \frac{y_i^T y_i}{y_i^T s_i}$ | $\frac{y_k^T y_k}{y_k^T s_k}$ |

TABLE 1. Values for different ζ_k and ζ_k^C used in Experiment 1.

4.5. Computational complexity. In this section, we consider the computational cost per iteration of Algorithm (1). The LDL^T factorization of $S_k^T S_k$ and $\Psi_k^T \Psi_k$ are each $\mathcal{O}(l^3)$. Moreover, if the LDL^T factorization is updated each iteration instead of computed from scratch, this cost drops to $\mathcal{O}(l^2)$. The spectral decomposition's dominant cost is at most $\mathcal{O}(l^3) = (l^2/n) \mathcal{O}(nl)$, depending on the rank of Ψ_k . Finally, the **obs** method requires two matrix-vector products with P_{\parallel} , whose dominant cost is $\mathcal{O}(4nl)$ flops to solve each trust-region subproblem. (For comparison, this is the same as the dominant cost of L-BFGS [18].)

5. NUMERICAL EXPERIMENTS

The results in this section are based on the performance of the MSS method on 60 large-scale unconstrained optimization problems from the CUTest test set [5] with $n \geq 1000$. For these experiments, the trust region was defined using the Euclidean norm, and Algorithms 1-2 were run with the following parameters: $\eta_1 = 0.01$, $\eta_2 = 0.75$, $\gamma_1 = 0.5$, $\gamma_2 = 2$, and $\gamma_p = 0.8$. Finally, the algorithm chose a multiple of the steepest descent direction as the step whenever the $\text{cond}(B) > \tau$, where $\tau = 10^{12}$, or $\|B\| > \hat{\tau}$, where $\hat{\tau} = 10^{15}$.

For these experiments, the MSS algorithm terminated successfully if iterate x_k satisfied

$$\|x_k\| \leq \max(\tau_g * \|g_0\|, \tau_g),$$

where $\tau_g = 1e^{-5}$ and $g_0 = g(x_0)$. On the other hand, the MSS method terminated unsuccessfully if either of the following occurred: the number of iterations reached $2n$, the number of function evaluations reached $100n$, or Δ became smaller than 100ϵ , where ϵ denotes machine precision.

Experiment 1. The first experiment compares the number of function evaluations needed to solve each problem using four different options for initializations (17) found in Table 1. Three memory size limits ($m = 3, 5$, and 7) were tested. Finally, the best options for each choice of memory were compared in a final performance profile. As mentioned in the discussion following Theorem 4, provided $\text{tr}(Y_k^T S_k) > 0$, ζ decreases the difference between $B_k S_k = Y_k$ in the Frobenius norm. We performed two sets of experiments: (i) updating s and y regardless of the sign of their inner product and (ii) updating s and y only when

$$s_i^T y_i > \epsilon \|s_i\| \|y_i\|, \quad (32)$$

where ϵ is machine precision. Case (ii) slightly outperformed case (i) on the final performance profile, without significant differences in the rest of the performance profiles. For brevity, we report only the performance profiles obtained by updating the pairs (s, y) when they satisfy (32).

The first initialization option tested is the Barzilai and Borwein (BB) initialization, which is a standard choice for many quasi-Newton methods [16]. This is a one-parameter initialization that does not use a dense initialization; however, we found that this is a very competitive initialization for the MSS method. The second option is the one-parameter initialization that picks both parameters to best satisfy the multiple secant equations (see Theorem 3). The third option is a two-parameter initialization is based on Theorem 4, which sets ζ_k to best satisfy the multiple secant equations. For this initialization, ζ_k^C was set as the BB initialization. Finally, the last option sets ζ_k to be the maximum ratio of $y_i^T y_i / y_i^T s_i$ where i ranges over the stored updates, and ζ_k^C is chosen as the BB initialization. This initialization is based on ideas in [17]. In all experiments, safeguarding was used to ensure that ζ_k and ζ_k^C were neither too large nor too small. Specifically, for these experiments, either parameter was set to its previous value if it fell outside the range $[10^{-4}, 10^4]$. In addition to preventing a parameter from becoming too large, this also prevents either parameter becoming negative leading to indefinite trust-region subproblems (see the discussion at the end of 3.2). Finally, for the initial iteration, $\zeta_0 = \zeta_0^C = 1$. The parameters chosen in Table 1 represent some of the best choices that we know of.

The results of Experiment 1 are summarized using performance profiles, proposed by Dolan and Moré[19]. Specifically, if \mathcal{P} denotes the set of test problems, the performance profiles plot the function $\pi_s : [0, r_M] \rightarrow \mathbb{R}^+$ defined by

$$\pi_s(\tau) = \frac{1}{|\mathcal{P}|} |\{p \in \mathcal{P} : \log_2(r_{p,s}) \leq \tau\}|,$$

where $r_{p,s}$ denotes the ratio of the number of function evaluations needed to solve problem p with method s with the least number of function evaluations needed to solve p by any method. Note that r_M is the maximum value of $\log_2(r_{p,s})$.

Figure 1 displays the results using three different memory sizes. The top left figure displays the results when the memory limit was set to 3. Initializing with Options 1 and 2, the MSS method converged on 58 problems; however, initialization with Options 3 and 4 converged on 59. The performance profile shows that the two-parameter initializations generally outperformed the one-parameter initializations. In the case of $m = 5$, the performance profile shows that the two-parameter initialization based on Theorem 4 outperforms the other initializations. It can be also argued that Option 4 is competitive with both one-parameter initializations. In this experiment, using each initialization the MSS method solved 59 out of 60 problems. Finally, in the case of $m = 7$, using each initialization the MSS method solved 58 out of 60 problems. In this case, Option 1 outperforms the two-parameter initializations. It is important to note that the MSS method performs the same number of function as gradient evaluations (i.e., one per iteration), and thus, the performance profile for gradient evaluations is identical to the ones presented for function evaluations.

In order to determine the best combination on this CUTEst test set, a second performance profile was generated that compared the best options for each choice of memory. Figure 2 suggests that the MSS method runs best using a fewer amount of stored pairs with a two-parameter initialization. In all cases, using $m = 7$ underperformed $m = 3$ and $m = 5$.

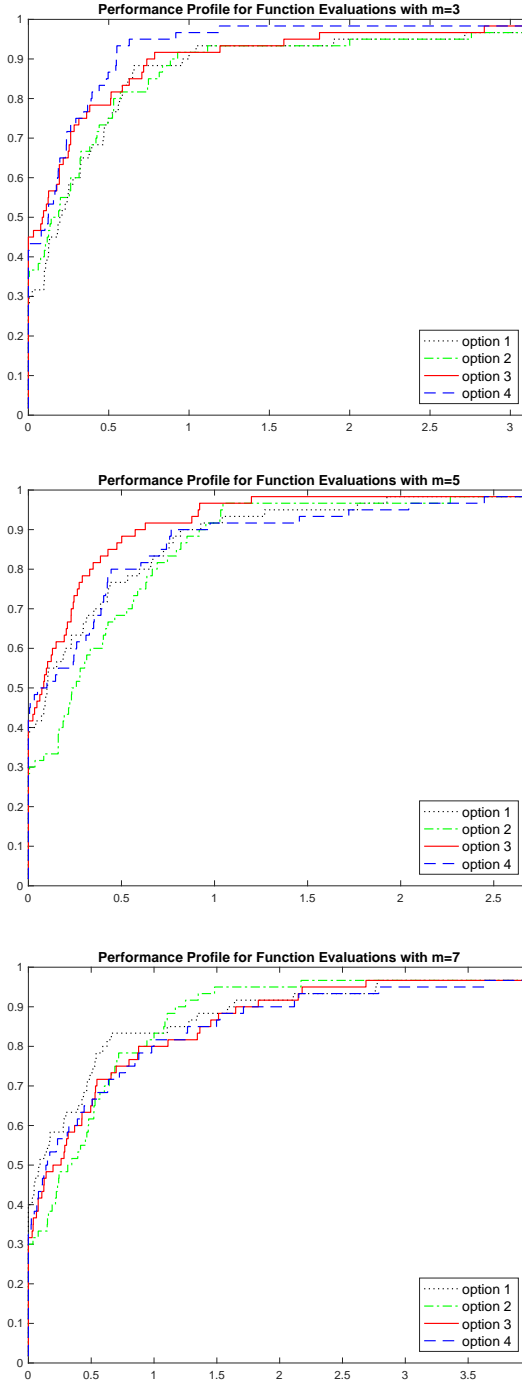


FIGURE 1. Performance profile comparing function evaluations using the initializations in Table 1 with $m = 3, 5$, and 7 .

Experiment 2. In this section, we compare the MSS method with a dense initialization to an L-SR1 method. The reason for this choice is that both methods generate approximations Hessians that may be indefinite, and thus, it is natural to use both in a trust-region framework. For this experiment, we implemented a standard L-SR1 trust-region method [8, Algorithm 6.2] and chose the approximate solution to the subproblem using a truncated-CG (see, for example, [8, 9]). The LSR-1 method was initialized using $B_0 = \gamma_k^{SR1} I$, where γ_k^{SR1} could be changed each

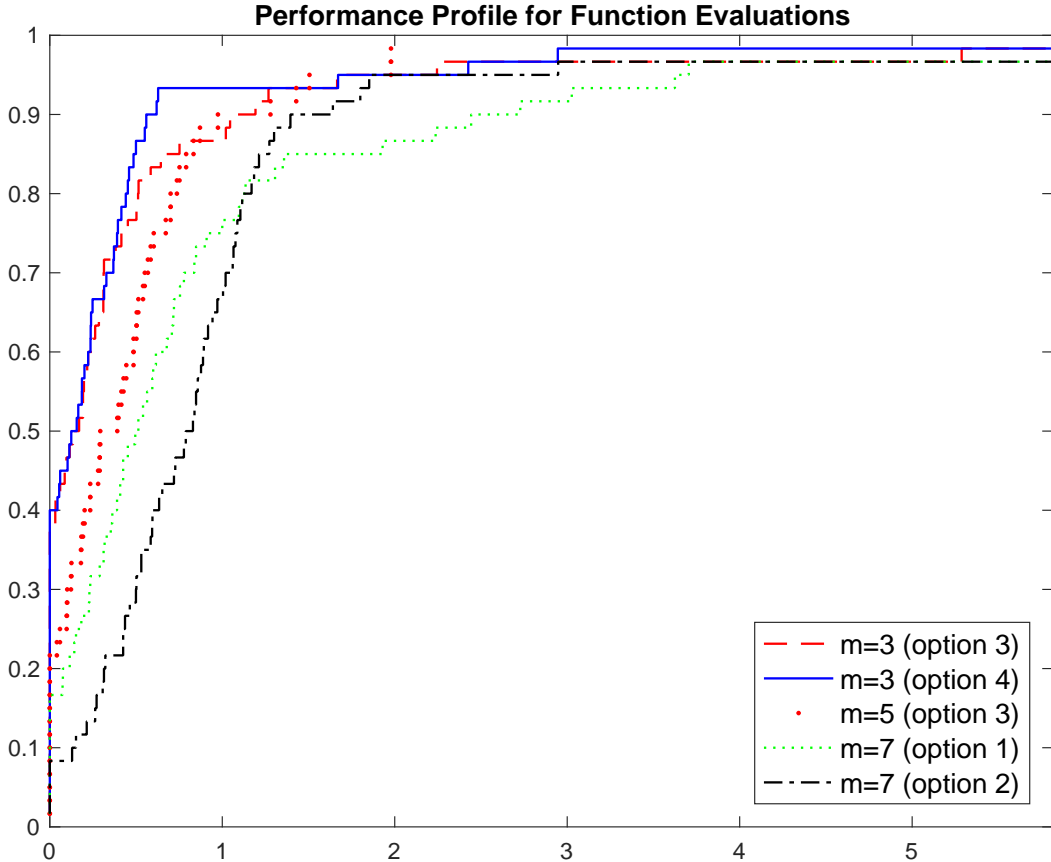


FIGURE 2. Performance profile comparing function evaluations using different memory sizes and initializations.

iteration. Updates to the quasi-Newton pairs were accepted provided

$$|s_k^T(y_k - B_k s_k)| \geq \tau_s \|y_k - B_k s_k\| \|s_k\|, \quad (33)$$

where $\tau_s = 1e^{-8}$. For these experiments, the initial iteration used $B_0 = I$, and for subsequent iterations, the LSR-1 method was initialized two ways: (1) using the BB initialization and (2) using $B_0 = I$ for every initialization. Since we require (33) to update the pairs, there was no danger of the denominator for the BB initialization becoming zero. For these results, the trust-region framework for the MSS and L-SR1 methods were identical. The results of this experiment are presented in a performance profile and table. Figure 3 contains the performance profile for the results. From the figure, it appears that MSS outperforms L-SR1 in terms of function evaluations using $m = 3$ with the initialization given by option 3 and $m = 5$ with the initialization given by option 4. The MSS method with $m = 3$ and option 4 as well as $m = 5$ and option 3 solved 59 out 60 problems. In contrast, L-SR1 with $m = 3$ using both initializations failed to converge on 5 problems. With $m = 5$ and the BB initialization, L-SR1 did not converge on 6 problems; with $m = 5$ and the identity initialization it failed to converge on 3 problems.

To better visualize the results, the data in Figure 3 was split into two performance profiles in Figure 4, grouped by memory size. In this figure, it is clear that for $m = 3$, the MSS method outperform the L-SR1 methods. For $m = 5$, MSS does

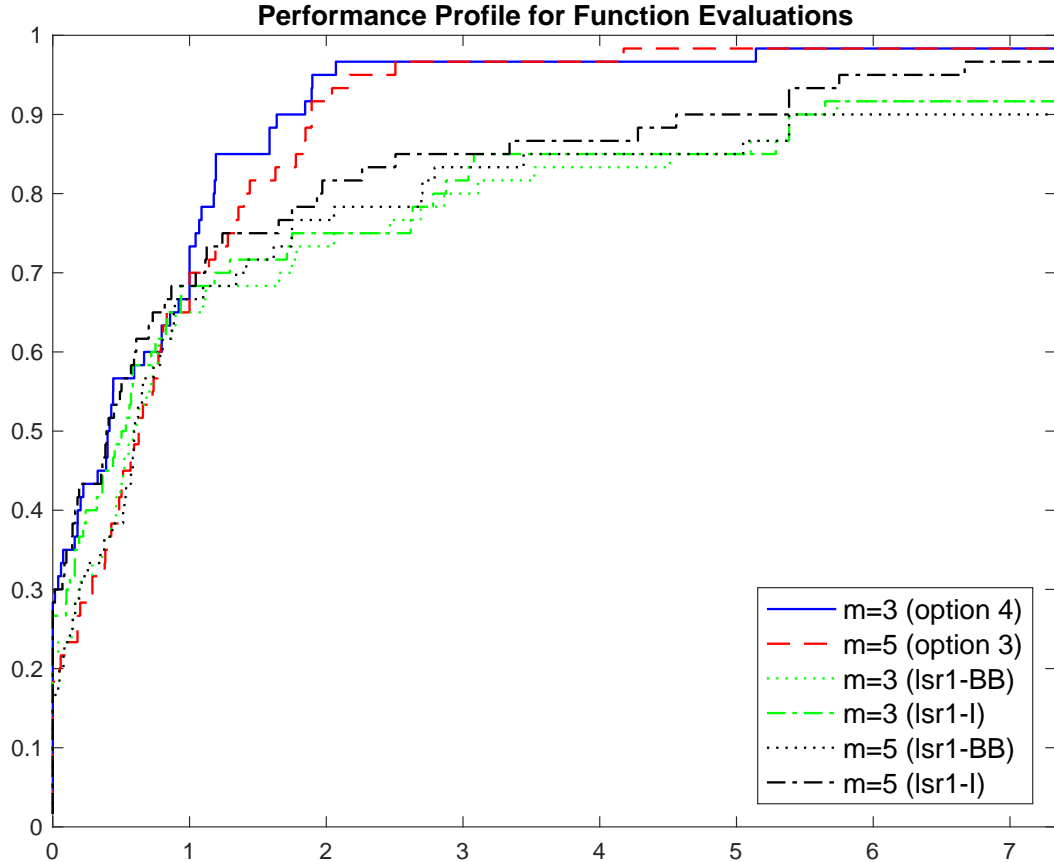


FIGURE 3. Performance profile comparing function evaluations using MSS with option 3, L-SR1 with the BB initialization, and L-SR1 with the $B_0 = I$.

not obviously outperform the L-SR1 methods as in the $m = 3$ case. However, it turns out that there is an important aspect of the results that is not captured in the performance profile. Of the 60 problems, there were 54 problems that all three methods solved. Table 2 presents the cumulative results for $m = 5$. The number of function evaluations reported in the table consider only the 54 problems on which all the methods converged. Despite the performance profile results, there is a substantial decrease in the number of function evaluations between the MSS method and the L-BFGS methods. Specifically, there was a 56.57% decrease and a 63.05% decrease if the MSS method is used instead of the L-SR1 with the BB initialization and the identity initialization, respectively. The reason why these results are not captured by the performance profile is that the MSS method achieved a very significant reduction in function evaluations on many problems when it outperformed the L-SR1 methods; in contrast, there were few problems where the L-SR1 methods significantly outperformed the MSS method.

As in the first experiment, both the MSS and L-SR1 trust-region methods require one function and one gradient evaluation per iteration; for this reason, the performance profiles for gradient evaluations is identical to the performance profiles reported in this section.

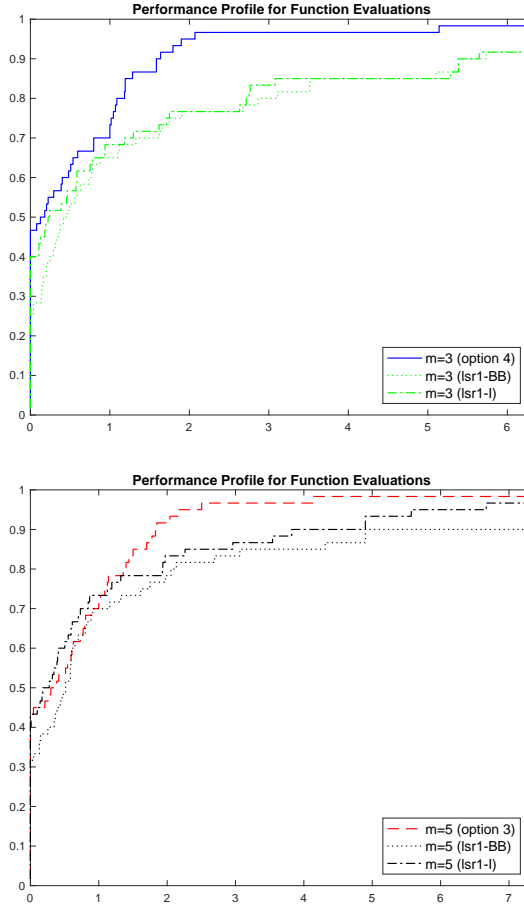


FIGURE 4. Performance profile with $m = 3$ (left) and $m = 5$ (right).

TABLE 2. Cumulative results on 60 CUTEst problems for $m = 5$.

| | MSS | SR1-BB | SR1-I |
|---------------------------|------|--------|--------|
| Problems solved | 49 | 54 | 58 |
| Function evaluations (FE) | 8753 | 20152 | 23066 |
| Improvement in FE | - | 56.57% | 62.05% |

Figure 5 compares the CPU time required by the MSS method and the two L-SR1 methods with $m = 3$. And, Figure 6 compares the CPU time required by the MSS method and the two L-SR1 methods with $m = 5$. These performance profiles indicates that the MSS method was significantly faster given the same memory size.

6. CONCLUDING REMARKS

In this paper, we demonstrated how a dense initialization can be used with a MSS method. In numerical experiments on CUTEst test problems, the dense initialization performs better than constant diagonal initializations. Results suggest that this method performs well with small memory sizes (i.e., $m = 3$ outperformed the other memory sizes and the number of function evaluations generally increased as m increased). Moreover, with small m , the proposed method generally outperforms a basic L-SR1 trust-region method. Further research includes considering other

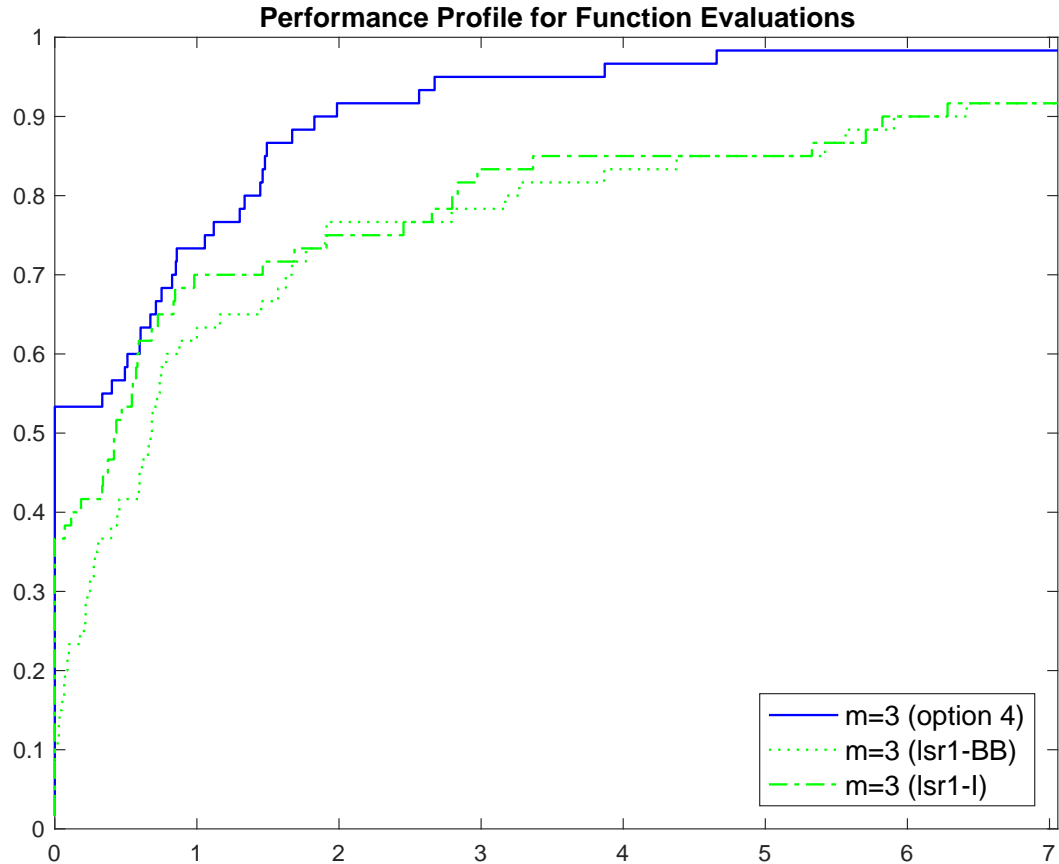


FIGURE 5. Performance profile comparing CPU time using $m = 3$ with MSS (option 3), L-SR1 with the BB initialization, and L-SR1 with the $B_0 = I$.

symmetrization, choices for the two parameters ζ and ζ^C , and trust-region norms (including the so-called *shape-changing norm* first proposed in [20]). The results of these investigations will be submitted as a second paper.

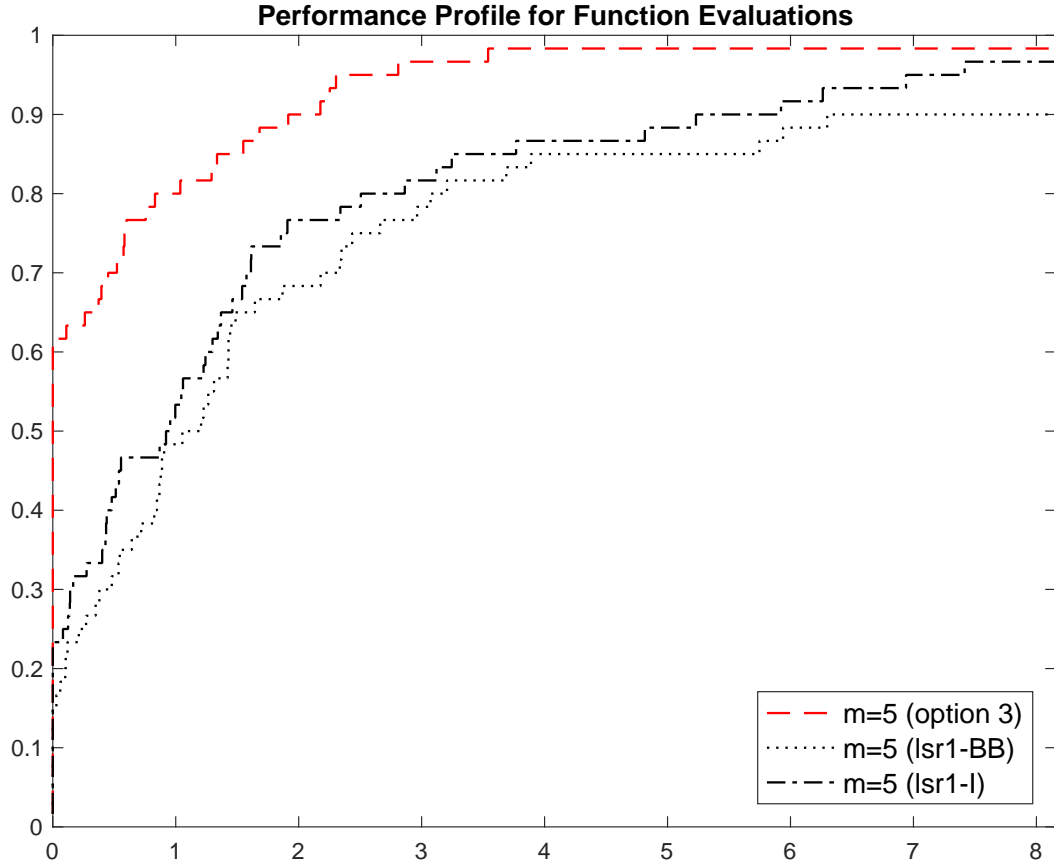


FIGURE 6. Performance profile comparing CPU time using $m = 5$ with MSS (option 3), L-SR1 with the BB initialization, and L-SR1 with the $B_0 = I$.

REFERENCES

- [1] OP Burdakov. Methods of the secant type for systems of equations with symmetric jacobian matrix. *Numerical functional analysis and optimization*, 6(2):183–195, 1983.
- [2] Oleg P Burdakov, José Mario Martínez, and Elvio A Pilotta. A limited-memory multipoint symmetric secant method for bound constrained optimization. *Annals of Operations Research*, 117(1-4):51–70, 2002.
- [3] Robert B Schnabel. Quasi-newton methods using multiple secant equations. Technical report, Colorado University at Boulder Department of Computer Science, 1983.
- [4] Johannes Brust, Oleg Burdakov, Jennifer B. Erway, and Roummel F. Marcia. A dense initialization for limited-memory quasi-Newton methods. *Computational Optimization and Applications*, 74(1):121–142, 2019.
- [5] Nicholas I. M. Gould, Dominique Orban, and Philippe L. Toint. Cutest: a constrained and unconstrained testing environment with safe threads for mathematical optimization. *Computational Optimization and Applications*, 60(3):545–557, 2015.
- [6] Johannes Joachim Brust. *Large-Scale Quasi-Newton Trust-Region Methods: High-Accuracy Solvers, Dense Initializations, and Extensions*. PhD thesis, UC Merced, 2018.
- [7] Richard H. Byrd, Jorge Nocedal, and Robert B. Schnabel. Representations of quasi-newton matrices and their use in limited memory methods. *Mathematical Programming*, 63(1):129–156, 1994.
- [8] Jorge Nocedal and Stephen Wright. *Numerical optimization*. Springer Science & Business Media, 2006.

- [9] Andrew R Conn, Nicholas IM Gould, and Philippe L Toint. *Trust region methods*. SIAM, 2000.
- [10] David M Gay. Computing optimal locally constrained steps. *SIAM Journal on Scientific and Statistical Computing*, 2(2):186–197, 1981.
- [11] Jorge J Moré and Danny C Sorensen. Computing a trust region step. *SIAM Journal on Scientific and Statistical Computing*, 4(3):553–572, 1983.
- [12] Jennifer B. Erway and Roummel F. Marcia. Algorithm 943: MSS: Matlab software for l-bfgs trust-region subproblems for large-scale optimization. *ACM Trans. Math. Softw.*, 40(4), 2014.
- [13] Oleg Burdakov, Lujin Gong, Spartak Zikrin, and Ya-xiang Yuan. On efficiently combining limited-memory and trust-region techniques. *Mathematical Programming Computation*, 9(1):101–134, 2017.
- [14] Johannes Brust, Jennifer B Erway, and Roummel F Marcia. On solving L-SR1 trust-region subproblems. *Computational Optimization and Applications*, 66(2):245–266, 2017.
- [15] Jennifer B Erway and Roummel F Marcia. On efficiently computing the eigenvalues of limited-memory quasi-Newton matrices. *SIAM Journal on Matrix Analysis and Applications*, 36:1338–1359, 2015.
- [16] J. Barzilai and J. Borwein. Two-point step size gradient methods. *IMA Journal of Numerical Analysis*, 8(1):141–148, 01 1988.
- [17] Johannes Brust, Oleg Burdakov, Jennifer Erway, and Roummel Marcia. Algorithm xxx: Sc-sr1: MATLAB software for solving shape-changing L-SR1 trust-region subproblems. Technical report, arXiv:1607.03533 [math.OC], 2021.
- [18] Jorge Nocedal. Updating quasi-newton matrices with limited storage. *Mathematics of Computation*, 35(151):773–782, 1980.
- [19] E. Dolan and J.J. Moré. Benchmarking optimization software with performance profiles. *Mathematical Programming*, 91:201–213, 2002.
- [20] O. Burdakov and Y.-X. Yuan. On limited-memory methods with shape changing trust region. In *Proceedings of the First International Conference on Optimization Methods and Software*, page p. 21, 2002.

Email address: erwayjb@wfu.edu

DEPARTMENT OF MATHEMATICS, WAKE FOREST UNIVERSITY, WINSTON-SALEM, NC 2 7109

Email address: rezapom@wfu.edu

DEPARTMENT OF MATHEMATICS, WAKE FOREST UNIVERSITY, WINSTON-SALEM, NC 2 7109